ELSEVIER

Ceramics International 25 (1999) 359–366

CERAMICS INTERNATIONAL

On the toughening mechanisms of SiC platelet-reinforced Al_2O_3/Y-TZP nano-ceramic matrix composites

C. Kaya [a,b,*], F. Kaya [a,b], P.A. Trusty [a], A.R. Boccaccini [c], M. Marsoglu [d]

[a] *IRC in Materials for High Performance Applications, The University of Birmingham, Edgbaston, Birmingham B15 2TT, UK*
[b] *School of Metallurgy and Materials, The University of Birmingham, Edgbaston, Birmingham B15 2TT, UK*
[c] *FG Werkstofftechnik, TU Ilmenau, D-98684 Ilmenau, Germany*
[d] *Department of Metallurgy and Materials, Yildiz Technical University, 80750, Besiktas, Istanbul, Turkey*

Received 5 March 1998; accepted 24 April 1998

Abstract

Al_2O_3 ceramic matrix composites toughened with 3Y-TZP (yttria-containing tetragonal zirconia polycrystals) and oriented hexagonal shape α-SiC platelets were fabricated using slip casting and cold isostatic pressing. The effect of platelet aspect ratio and volume fraction on fracture toughness, and mode and microstructure of the final composite was examined. The fracture toughness of the reinforced-composites was evaluated using indentation in four-point bending test. Scanning electron microscopy and transmission electron microscopy were used to determine the microstructural details and dominant toughening mechanisms which occurred. Toughness measurement tests and detailed observations of microstructures and fracture surface profiles have led to the conclusion that multiple-toughening behaviour via transformation toughening, microcracking, crack deflection, load transfer and platelet debonding and pull-out, as well as thermal residual stresses have a significant contribution in improving the fracture toughness. A fracture toughness value as high as 11.2 MPa $m^{1/2}$ was achieved for the specimens sintered at 1600°C for 3 h with a platelet addition of 30 vol%.

Keywords: B. Failure analysis; B. Microstructure-final; C. Toughness and toughening; Al_2O_3/Y-TZP ceramic composite

1. Introduction

Microstructural development of brittle matrix materials, such as ceramics [1–4] or glass ceramics [5,6] via second phase addition needs a better understanding of the toughening mechanisms which control the mechanical response of the final component. One strategy in obtaining tough and reliable ceramic composites is the addition of a high-modulus, high strength and high ductility second phase in the form of platelets/particulates, to a low-modules, low strength, brittle ceramic matrix. Experimental studies and models indicate that the toughening improvement by a dispersed highly anisotropic platelet addition is based on the contribution of several mechanisms, including debonding, pull-out (platelet sliding) [7], crack bridging [8], microcrack formation [9,10] and crack deflection [11] at the platelet-matrix interface, load transfer, as well as thermal residual stresses [12]. The critical characteristics of the matrix-platelet interface can be summarised in terms of low interfacial fracture energy and moderate interfacial sliding resistance after debonding [13]. A number of factors, such as platelet aspect ratio, orientation and volume fraction should be taken into account when a platelet reinforced component is designed for use in engineering applications. Furthermore, when the platelet/particulate phase has a higher thermal expansion coefficient than the matrix, the average thermal stresses in the particulates are in tension while they are in compression in the matrix. In that case, when the toughness of a particulate/platelet-reinforced ceramic component is estimated, the effect of the thermal residual stresses have to be taken into consideration as they can aid the debonding/crack deflection mechanism, and hence, multiple-toughening behaviour in particulate/platelet or whisker reinforced ceramic composites [14].

In this study, an Al_2O_3/Y-TZP (yttria-containing tetragonal zirconia polycrystals) ceramic composite was chosen as a matrix due to its excellent mechanical

* Corresponding author.

0272-8842/99/$20.00
PII: S0272-8842(98)00052-2

properties [15–17]. SiC platelets were chosen as the reinforcing additive, because, there are only a limited amount of data in the literature on SiC platelet reinforced-Al_2O_3/Y-TZP ceramic systems which show multiple toughening behaviour. SiC platelets have been used, however, to reinforce alumina [18], alumina-TZP composite [19,20], mullite [21], zirconia [22], SiC [23], and Si_3N_4, [24] ceramics. The potential advantages of platelets over particulate reinforced systems include more effective crack deflection and enhanced load-carrying capacity. In addition, other toughening mechanisms such as crack bridging and pullout are possible. The multiple toughening behaviour associated with both zirconia and platelet additions will be examined in this work with emphasis on the effect of thermal residual stresses on the fracture toughness as they are the main precursor to the debonding, pull-out and crack deflection mechanisms which increase the fracture toughness of the final component.

2. Experimental methods

2.1. Materials and composite preparation

The composite preparation has been reported in detail previously [20]. Briefly, an α-Al_2O_3 powder (Alcoa A-16 SG, mean particle size 0.3 gm) doped with 0.05 wt% MgO as a sintering additive to increase the sinterability and 20 vol% ZrO_2 (BDH Chemicals, UK, mean particle size 0.4 μm) stabilised with 3 vol% Y_2O_3 ceramic powders were first ball-milled in deionised water together with high purity alumina and zirconia balls for 24 h. A kinetically stable slip was obtained at a pH value of 4.5 using Darvan C and surfynol as deflocculant and surfactant, respectively to obtain a homogeneous suspension and eliminate the inclusion size effect during sintering [25]. Hexagonal α-SiC in the form of platelets (Third Millennium Materials Inc., USA, -400 mesh grade) having different mean aspect ratios (3, 8 and 12) was used as a reinforcing additive. Five different slips containing 0, 10, 20, 30 and 40 vol% of SiC platelets were prepared for each aspect ratio to investigate their effect on the mechanical properties. The solids-content of all the slips was 60 wt%. Slip casting was chosen as a wet colloidal processing technique to obtain consolidated bodies and slip-cast specimens which could be compacted further using cold isostatic pressing at 400 MPa for 5 min. The dried samples were sintered in a $MoSi_2$ resistance furnace in flowing nitrogen at 1600°C for 3 h.

2.2. Fracture toughness determination

Indentation strength in four-point bending (ISB) was chosen to estimate the fracture toughness using a formula reported in the literature [26]:

$$K_{IC} = \eta(E/H)^{1/8}(\sigma_f P^{1/3})^{3/4} \quad (2)$$

where K_{IC} is the fracture toughness, E is Youngs modulus, H is the Vickers hardness, η is a geometrical constant (0.59 as suggested in the literature [27]), σ_f is the fracture strength and P is the indentation load. The four-point bend strength and Young's modulus of each specimen were measured with an Instron testing machine with a 25 mm inner and 35 mm outer span and a cross-head speed of 0.5 mm/min. A special four-point bend fixture comprising tiltable, free-rolling pins and an adjustable span position was used to minimise sources of error, such as unequal moments (due to unequal load distributions), specimen twisting, wedging and frictional forces at the knife edges. All the surfaces to be indented were polished with 3, 1 and 0.25 μm diamond pastes. Polished surfaces were indented using a load of 294 N for K_{IC}, measurements. Indented samples were fractured in the four-point bend test described above. The fracture toughness values are expected to be different in different directions due to the anisotropic character of the microstructure [13]. K_{IC} values reported here were calculated based on the indented planes, in which the platelets oriented on their edges. In this case, the indentation cracks propagate parallel and perpendicular to the platelet edges in all propagation directions.

2.3. Microstructural observations

Microstructural observations were carried out using scanning electron microscopy (Jeol 5410 and field emission gun Hitachi S-4000) and transmission electron microscopy (Philips CM 20 TEM and Jeol FX-4000 TEM). SEM observations were used for general microstructural characterisation, and to study also the crack profiles of pre-notched and fractured specimens. For the TEM observations, prepared TEM foils were coated with a very thin C-layer to prevent electron charging during observations.

3. Results and discussion

The fracture toughness of SiC platelet reinforced Al_2O_3/Y-TZP composites as a function of platelet volume fraction for different aspect ratios is shown in Fig. 1. The maximum value of K_{IC} was determined as 11.2 MPa $m^{1/2}$ for a composite containing 30 vol% of platelets, compared with 7.4 MPa $m^{1/2}$ for the unreinforced Al_2O_3/Y-TZP composite. The main contributions to the improvement of K_{IC} can be attributed to the tetragonal to monoclinic phase transformation of the zirconia particles and the toughening mechanisms such as crack deflection which are promoted by the presence of the platelets. Fig. 2 shows SEM micrographs of the fracture surfaces of an unreinforced and a 30 vol%

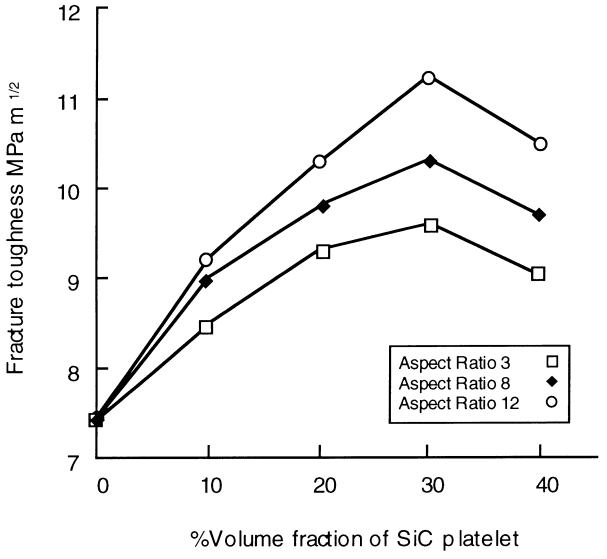

Fig. 1. Fracture toughness of SiC platelet reinforced Al_2O_3/Y-TZP composite as a function of platelet volume fraction for different aspect ratios.

platelet-reinforced composite. As can be seen, in both cases the fracture mode is intergranular.

Toughness improvement (ΔK^c) in zirconia-based ceramics due to transformation toughening is estimated using the following formula reported in the literature [28]:

$$\Delta K^c = \gamma E e^T v^T w^{1/2} \quad (5)$$

where γ is a constant, E is the Young's modulus of the composite, e^T is the transformation stress, v^T is the volume fraction of transformable tetragonal zirconia, and w is the size of transformation zone. From this equation, it is expected that increasing the transformation zone which can be increased by increasing the matrix toughness results in a higher ΔK^c value. With the present system, if the Al_2O_3/SiC platelet composite is considered as the matrix and the TZP particles as the reinforcing addition, the fracture toughness of the matrix increases with increasing platelet addition so that the radius of the transformation zone is increased and tetragonal zirconia can transform to monoclinic zirconia due to thermal tensile stresses [29].

The relative amounts of monoclinic zirconia in unreinforced and reinforced composites was calculated from the XRD peaks using the following formula reported in the literature [30]:

$$V_m = \frac{I_m(111) + I_m(11\bar{1})}{I_t(111) + I_m(111) + I_m(11\bar{1})} \times 100 \quad (3)$$

$$V_t = 1 - V_m \quad (4)$$

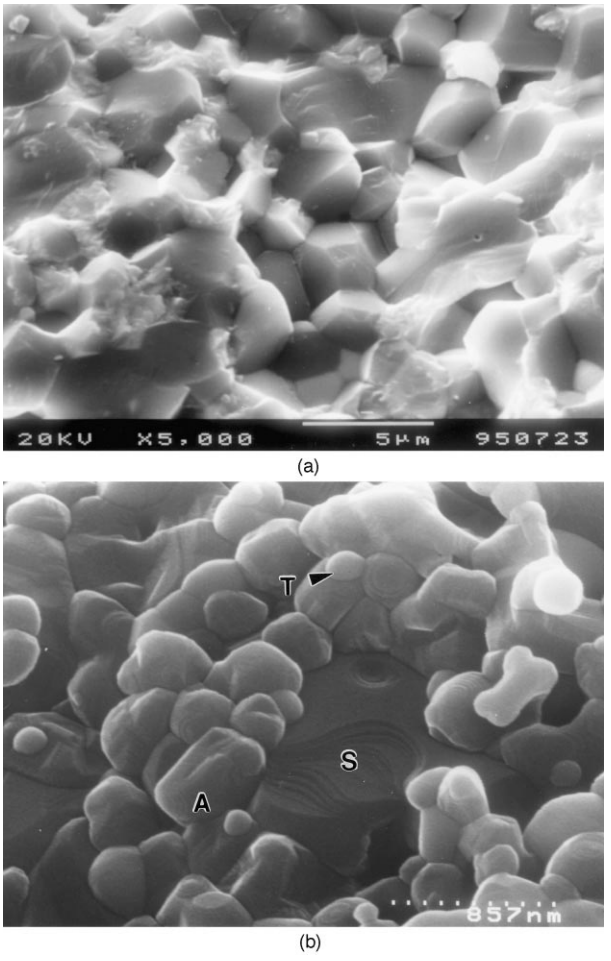

Fig. 2. Scanning electron micrographs of the fracture surfaces of SiC platelet-reinforced Al_2O_3/Y-TZP composites showing the effect of platelet loading on fracture characteristics. (a) 0 vol% (intergranular and transgranular fracture), and (b) 30 vol% of platelets (intergranular fracture). Note T: TZP, A: Alumina, S: SiC.

Table 1
Effect of SiC platelet addition on the amount of transformed monoclinic zirconia present in Al_2O_3/Y-TZP 'matrix' material

Volume % of SiC added to Al_2O_3/Y-TZP	$E_{composite}$ (GPa) (measured)	% monoclinic ZrO_2	
		Polished surface	Fracture surface
0	295	67	81
10	325	27	55
20	340	23	51
30	360	21	48
40	395	17	37

where V_m and V_t are the volume fractions of monoclinic and tetragonal zirconia, respectively, and $I_m[(111), (11\bar{1})]$ and $I_t(111)$ are the intensity of the diffracted beams from the (111) planes of monoclinic and tetragonal zirconia phases, respectively. Table 1 shows the amount of observed monoclinic zirconia present on the fracture surfaces for each of the composites tested. As

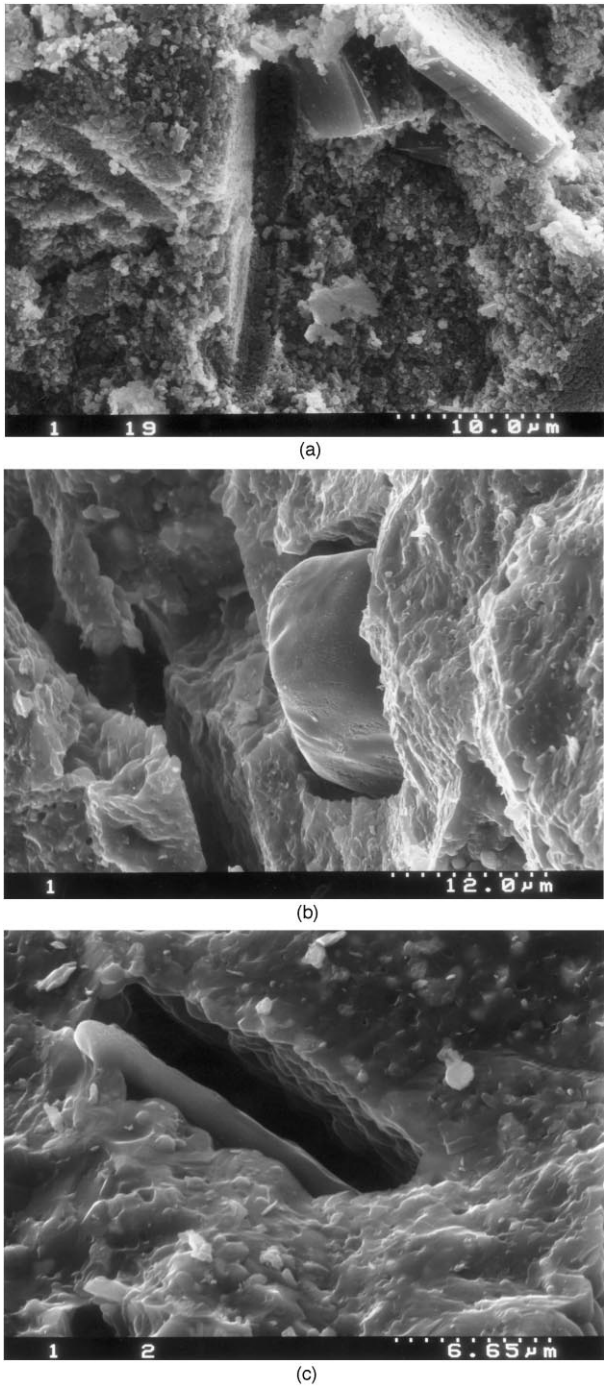

Fig. 3. High resolution (SEM) micrographs of the fracture surfaces of SiC platelet-reinforced Al_2O_3/Y-TZP composite showing: (a) debonding/sliding; (b) crack deflection; (c) pull-out mechanisms which occur during composite failure.

can be seen from this Table, the volume fraction of monoclinic zirconia phase on the fracture surface decreases as the volume fraction of platelets is increased. This indicates that the transformation zone size actually decreased. It is assumed that the modulus load transfer by the platelets acts to lower the effective shear stress at the crack tip, and this leads to less zirconia transforming to the monoclinic phase at the fracture surface [31]. Hence, the role played by the transformation toughening effect of the zirconia phase becomes less pronounced with increasing platelet addition and at higher platelet volume fractions, crack deflection and modulus load transfer mechanisms become the dominant factors in improving the fracture toughness of the composite.

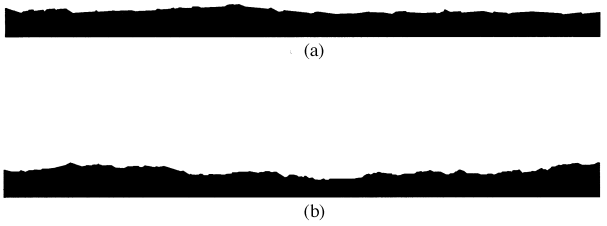

Fig. 4. Computer-generated schematic reconstruction of the surface roughness in: (a) Al_2O_3/Y-TZP 'matrix'; and (b) 30% vol. SiC platelet-reinforced Al_2O_3/Y-TZP 'composite'. Note the data was collated from experimental observations.

Residual thermal stresses are created at the platelet/matrix interface during cooling from the sintering temperature due to the thermal expansion mismatch between the SiC platelets ($\alpha = 4\times10^{-6}$/K), and the phases of the matrix: Al_2O_3 ($\alpha = 8\times10^{-6}$/K) and Y-TZP ($\alpha = 10\times10^{-6}$/K). Since $\alpha_{matrix} > \alpha_{platelet}$, it is expected that the SiC platelets are subjected to a compressive stress and the Al_2O_3/Y-TZP matrix to tangential tensile stresses, resulting in radial microcracks around the platelets. These microcracks increase the propensity for the occurrence of toughening mechanisms such as grain bridging [32]. Furthermore, the bonding between matrix and platelets is weak enough (due to thermal expansion mismatches between the matrix and platelets) to promote debonding/sliding and pull-out mechanisms as observed in Fig. 3.

An additional improvement in toughness is derived from modulus-load transfer. It is observed that the Young's modulus of the platelet reinforced composites increases with increasing volume fraction of platelet, i.e. value of 295 and 390 GPa for the unreinforced composite and for a composite reinforced with 40 vol% of platelets, respectively were measured (Table 1). In modulus load transfer, the stress at the crack tip is transferred along the high modulus platelets present in the composite to regions further away from the crack plane. In this way, the stress intensity at the crack tip is reduced, leading to a subsequent increase in toughness.

3.1. Fracture surface roughness

The roughness profiles of the fracture surfaces of an Al_2O_3/Y-TZP 'matrix' and an Al_2O_3/Y-TZP 'composite' reinforced with 30 vol% platelets specimens are shown in a quantitative manner in Fig. 4. The collated data used to recreate these profiles can be displayed in

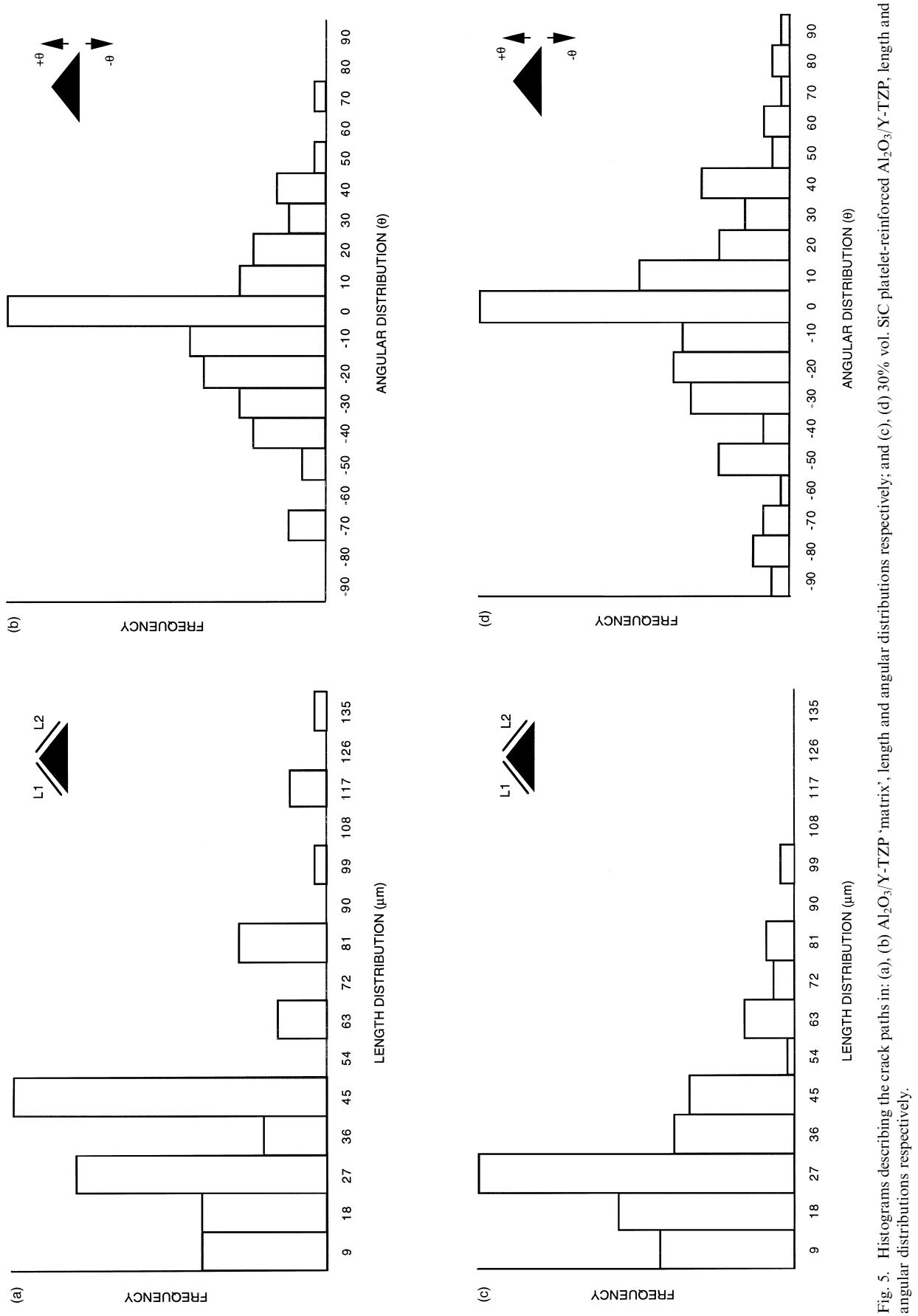

Fig. 5. Histograms describing the crack paths in: (a), (b) Al_2O_3/Y-TZP 'matrix', length and angular distributions respectively; and (c), (d) 30% vol. SiC platelet-reinforced Al_2O_3/Y-TZP, length and angular distributions respectively.

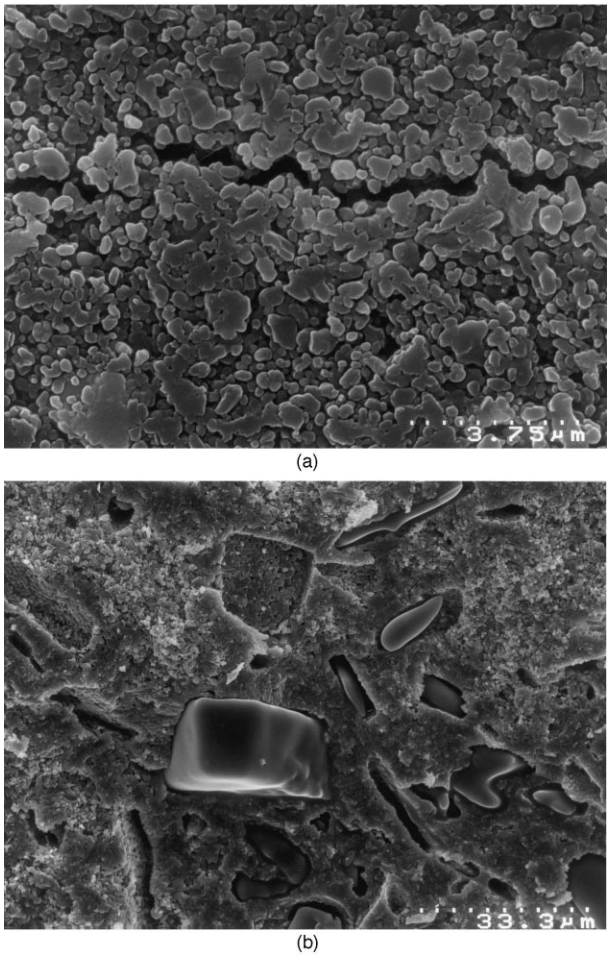

Fig. 6. SEM micrographs of surface roughness profiles due to crack deflection-initiated processes. (a) Side view of crack path in Al_2O_3/Y-TZP material showing minor crack deflections; (b) planar view of platelets on the surface of 30% vol. SiC platelet-reinforced Al_2O_3/Y-TZP which promote major crack deflections.

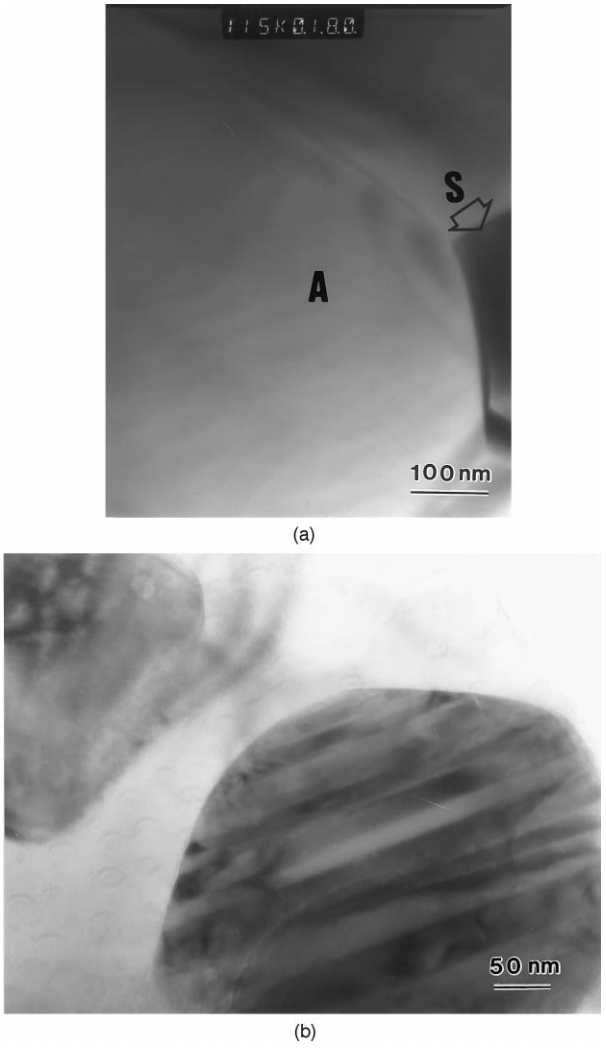

Fig. 7. Bright field transmission electron microscopy (TEM) micrographs indicating the detailed microstructure of SiC platelet-reinforced Al_2O_3/Y-TZP composite: (a) location of the platelet on the matrix grain boundaries. Note the weak interface between the matrix and SiC platelet (S: SiC, A: alumina); (b) the transformed monoclinic zirconia grain having a twin structure after fracture.

terms of the angular deviation of the crack as it traverses the specimen and the length of each crack segment prior to deviation. In this way, the data enable a comparison to be made between different materials. Fracture mechanics models predict that the toughening associated with crack deflection should be particle size invariant, but dependent highly on the morphology of the deflecting phase [11]. Histograms depicting these phenomena are shown in Fig. 5. Considering the length distribution of the 'matrix' (Fig. 5a), it can be seen that the most frequent distance traversed prior to crack deviation was in the 18 to 27 μm region and the longest recorded distance was 99 μm. Fig. 5b shows that the most frequent angle of deviation was between 0 and 10° and also that there were very few deviation angles above 40°. The lack of major crack deflections out of the plane of the advancing crack reduces also the propensity for other toughening mechanisms such as crack bridging or intergranular friction to be initiated. Hence, the increase in toughness of this 'matrix' is due mainly to the tetragonal to monoclinic transformation of the zirconia rather than to crack deflection initiated processes. Direct SEM observations of the crack path (Fig. 6a) have reiterated these findings in that they show that minimal crack deviations occur and that the fracture mode is mostly intergranular (brittle fracture), with the occurrence of some transgranular fracture also.

The length distribution histogram of the 'composite' (Fig. 5c), however, has an overall shape which is different from that of the matrix and this difference can be attributed solely to the presence of the platelets. During crack propagation in this 'composite', the crack is able to traverse the Al_2O_3/Y-TZP regions in a similar manner as with the previously described matrix case; but the presence of the larger platelets has caused the crack to

deflect at the platelet-matrix interface and travel much longer distances prior to a subsequent deviation. This is borne out in the histogram in that the longer 36–45 μm crack length range is the most frequent in this 'composite', and that distances as high as 135 μm prior to deviation have been recorded also. Considering the angular deviations in the composite (Fig. 5d), the basic shape of this histogram is similar to the angular distribution histogram of the matrix. In this case, however, the crack front meandering is affected by the presence of the hexagonal platelets. With the irregular shape and spatial distribution of the platelets, the angular deviations are far more pronounced than with the matrix. This has led to a greater amount of angular deviations being recorded between 40 and 90°, which is indicative of an increased amount of re-entrant angle crack deflection. As it has already been stated that transformation toughening effect of the zirconia is reduced in the composite systems, the high toughness in this system can be attributed more to crack deflection initiated processes [33]. Pezzotti has modelled the actual contribution of crack deflection in toughening and concluded that crack deflection as a toughening mechanism itself is generally small ($<40\%$ in terms of K_{IC} increase) even when maximum deflection can be achieved [34]. Fig. 6b shows a plan view of a fracture surface for a composite reinforced with 30 vol% of platelets. The presence of the platelets can be seen to increase the surface roughness, and hence, extent of crack deflection for this material. Assuming the presence of these platelets has increased the 'matrix' toughness (7.4 MPa $m^{1/2}$) by the maximum value of 40%, the 'composite' should have a toughness of 10.36 MPa $m^{1/2}$. The fact that the measured toughness for this system was 11.2 MPa $m^{1/2}$, shows that additional toughening mechanisms are operative. These include the transformation toughening of the zirconia phase, as well as pullout and modulus load transfer mechanisms.

Fig. 7 shows a TEM microstructure of the Al_2O_3/Y-TZP composite reinforced with 30 vol% of SiC platelets prepared from a sample sintered at 1600°C for 3 h. As can be seen, SiC platelets were located mainly on the grain boundary (see also Fig. 2b) and there is no reaction and, hence, reaction product at the platelet/matrix interface indicating a weak interfacial bond (Fig. 7a). This weak interface, therefore, supplies an ideal structure to promote platelet debonding/sliding and hence, crack deflection as well as pull-out mechanisms, as the fracture surface observations indicated. Fig. 7b shows the clear indications of a transformed monoclinic zirconia grain having twin structure. This shows that some transformation toughening is still occurring in the SiC platelet-containing composites. The TEM micrograph in Fig. 8 shows the presence of extensive dislocations within the platelets. According to Zhan et al. [35], who observed this phenomenon in their TiC reinforced

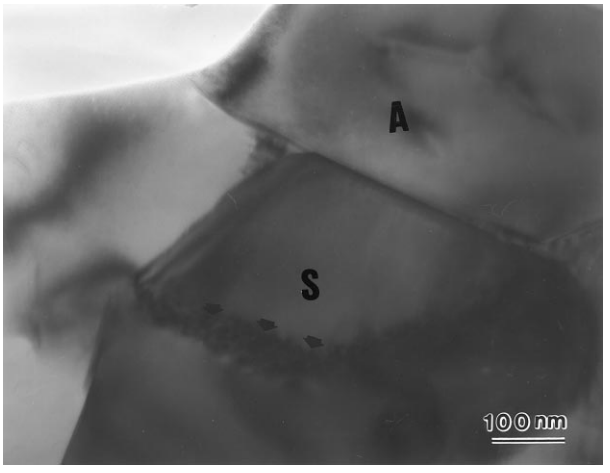

Fig. 8. Bright Field transmission electron micrograph of SiC platelet-reinforced Al_2O_3/Y-TZP composite showing the location of dislocations within the platelets (as arrowed) and a clear indication of the weak interface between the platelet and matrix.

Y-TZP system, this indicates that the mechanism of the momentary pinning of the moving crack front by the SiC platelets (i.e. crack bowing) may be an additional operative toughening mechanism.

4. Conclusions

The complex and multiple toughening mechanisms in SiC platelet reinforced Al_2O_3/Y-TZP ceramic composite were analysed using both high resolution and transmission electron microscopy together with fracture toughness measurement. At lower platelets loadings, phase transformation toughening and microcracking associated with zirconia particles can be combined with platelet reinforcement to achieve additional improvements in fracture resistance. However, the degree of contribution of each toughening mechanism in increasing the toughness of the composite is different depending on the platelet volume fraction. The crack deflection mechanism is found to be the most dominant factor at higher platelet additions in increasing the toughness of the composite whilst the transformation toughening contribution is reduced. Studies of propagating crack paths in pre-notched specimens have been able to quantify the extent of intergranular crack deflection for specimens with different platelet volume fraction additions. A significant contribution in increasing the toughness is derived also from load transfer by the platelets, pull-out/debonding, microcracking, crack bowing and thermal residual stresses. These mechanisms have all contributed synergistically to the fracture toughness value of 11.2 MPa $m^{1/2}$ which was recorded for a specimen containing 30 vol% of platelets and sintered at 1600°C for 3 h.

Acknowledgements

We would like to thank Third Millennium Materials Inc. for supplying the platelet samples and Yildiz Technical University Research Fund for financial support under contract number 94-A-07-02-03.

References

[1] M.N. Rahaman, Mater. Res. Soc. Symp. Proc. 249 (1992) 465–473.
[2] P.F. Becher, J. Am. Ceram. Soc. 74 (1991) 255–269.
[3] M.F. Ashby, Acta Metall. Mater. 41 (1993) 1313–1335.
[4] G. Sanders, M.V. Swain, Materials Forum 14 (1990) 60–69.
[5] A.R. Boccaccini, Ceram. Acta. 8 (1996) 5–10.
[6] A.R. Boccaccini, D.H. Pearce, P.A. Trusty, Composites Part A 28A (1997) 505–510.
[7] R. Janssen, K.H. Heussner, Powder Metall. Int. 23 (1991) 242–245.
[8] Y.S. Chou, D.J. Green, J. Am. Ceram. Soc. 76 (1993) 1985–1992.
[9] M. Rühle, A.G. Evans, R.M. McMeeking, P.G. Charalambides, Acta Metall. 35 (1987) 2701–2710.
[10] J.W. Hutchinson, Acta Metall. 35 (1987) 1605–1619.
[11] K.T. Faber, A.G. Evans, Acta Metall. 31 (1983) 565–576.
[12] M. Taya, S. Hayashi, A. Kobayashi, H.S. Yoon, J. Am. Ceram. Soc. 73 (1990) 1382–1391.
[13] Y.S. Chou, D.J. Green, J. Am. Ceram. Soc. 75 (1992) 3346–3352.
[14] P.F. Becher, T.N. Tiegs, J. Am. Ceram. Soc. 70 (1987) 651–654.
[15] R.C. Garvie, R. Hannink, R.T. Pascoe, Nature (London) 258 (1975) 703.
[16] F.F. Lange, J. Mater. Sci. 17 (1982) 225.
[17] L. Shi, B.S. Li, T.S. Yen, J. Mater. Sci. 31 (1993) 4019–4022.
[18] Y.S. Chou, D.J. Green, J. Am. Ceram. Soc. 76 (1990) 1985–1991.
[19] C. Kaya, F. Kaya, M. Marsoglu, J. Mater. Sci. Lett. 16 (1997) 892–896.
[20] Kaya, C., Kaya, F., Marsoglu, M., Mater. Sci. Engn. A247 (1998) 75–80.
[21] N. Kapuri, K.N. Rai, G.S. Upadhyaya, J. Mater. Sci. 31 (1996) 1481–1487.
[22] X. Miao, W.M. Rainforth, W.E. Lee, J. Eur. Ceram. Soc. 17 (1997) 913–920.
[23] R. Lenk, J. Adler, J. Eur. Ceram. Soc. 17 (1997) 197–202.
[24] B.T. Lee, G. Pezzotti, K. Hiraga, Mater. Sci. Engn. A. 177 (1994) 151–160.
[25] R. McMeeking, A.G. Evans, J. Am. Ceram. Soc. 65 (1982) 242.
[26] G.R. Anstis, P. Chantikul, B.R. Lawn, D.B. Marshall, J. Am. Ceram. Soc. 64 (1985) 539.
[27] A.G. Evans, Fracture 1 (1977) 529.
[28] A.G. Evans, R.M. Cannon, Acta Metall. 34 (1986) 761.
[29] G.Y. Lin, T.C. Lei, Y. Zhou, J. Mater. Sci. 15 (1996) 1267.
[30] R.C. Garvie, R. Hannink, M.V. Swain, J. Mater. Sci. 1 (1982) 437–440.
[31] K.-H. Heussner, N. Claussen, J. Europ. Ceram. Soc. 5 (1989) 193–200.
[32] A.G. Evans, J. Am. Ceram. Soc. 65 (1982) 127.
[33] M.C. Fredel, A.R. Boccaccini, J. Mater. Sci. 311 (1996) 4375–4380.
[34] G. Pezzotti, Acta Metall. 41 (1993) 1825.
[35] G.-D. Zhan, T.-R. Lai, J.-L. Shi, T.-S. Yen, Y. Zhou, Y.-Z. Zhang, J. Mater. Sci. 31 (1996) 2903–2907.